

Interplay between valley polarization and electron-electron interaction in a graphene ring

D. S. L. Abergel,^{1,*} Vadim M. Apalkov,² and Tapash Chakraborty^{1,†}

¹*Department of Physics and Astronomy, University of Manitoba, Winnipeg, Manitoba, Canada R3T 2N2*

²*Department of Physics and Astronomy, Georgia State University, Atlanta, Georgia 30303, USA*

(Received 12 September 2008; published 21 November 2008)

We have studied the interplay of valley polarization and the Coulomb interaction on the energy spectrum, persistent current, and optical absorption of a graphene quantum ring. We show that the interaction has a dramatic effect on the nature of the ground state as a function of the magnetic flux and that the absence of exchange interaction between electrons in opposite valleys means that the singlet-triplet degeneracy is not lifted for certain few-electron states. The additional energy-level crossings (fractional flux periodicity) due to the interaction directly lead to extra steps in the persistent current and intricate structures in the absorption spectrum that should be experimentally observable. By varying the width of the ring, the nature of the ground state at zero field can be varied and this is manifest in the measurable properties we discuss.

DOI: 10.1103/PhysRevB.78.193405

PACS number(s): 78.40.Ri, 73.43.Lp, 78.67.-n

Graphene (a single layer of carbon atoms arranged in a honeycomb lattice) with its unusual electronic properties has claimed the center stage of condensed-matter research for the past three years.¹ Theoretically investigated sixty years ago,² interest in this system widened after free-standing graphene flakes were obtained experimentally by Geim *et al.*³ in 2004. The linear band structure predicted for this material has been verified, and several striking experimental observations have been made, including the “half-integer” quantum Hall effect and a solid-state manifestation of the Klein paradox for massless Dirac fermions.

In neutral bulk graphene, the Fermi energy is located at the two inequivalent K points, and the corresponding pairs of single-particle eigenstates in each of these “valleys” are degenerate with each other. An experimental observation⁴ of lifting of this valley degeneracy in high-field quantum Hall effect measurements has prompted several theoretical studies seeking the origin of this valley polarization.⁵ The intriguing possibility of controlling the energy difference between electron states in opposite valleys which would facilitate the idea of valleytronics (utilizing the valley quantum number to control the system) would be an exciting development.

Quantum rings of nanoscale dimensions are known to carry a persistent current: an equilibrium current driven by the magnetic field threading the ring.⁶ This is a direct consequence of the Aharonov-Bohm (AB) effect⁷ which manifests itself as periodic oscillations in the energy spectrum of the electronic system as a function of the number of flux quanta threading the ring.⁸ Impressive progress in fabricating nanosize quantum rings containing only a few electrons has led to equally notable results on the observation of the properties of energy spectra, first noticed in Ref. 8, via magnetoabsorption spectroscopy⁹ and in magnetotransport measurements.¹⁰ The important role of the electron-electron interaction in this system was found to lift the degeneracy between states with different spin as a means to gain the exchange energy.¹¹ A direct consequence of this is the fractional flux periodicity that was indeed observed in subsequent experiments on semiconductor quantum rings containing only about four electrons.¹²

Graphene rings have recently been fabricated and AB oscillations were observed in their conductance.¹³ The com-

bined effect of the ring confinement and applied magnetic flux is suggested theoretically to lift the orbital degeneracy arising from the two valleys in a controllable way.¹⁴ Further, a ring with quantum point contacts has been shown to polarize the transport current with respect to the valley.¹⁵ The important effects of the Coulomb interaction on the valley degeneracy and ground-state properties have not yet been investigated.

In this work, we report on the effect of the Coulomb interaction on the energy spectrum, persistent current, and optical-absorption spectrum of a graphene quantum ring. We show that the interaction, the total valley quantum number, and the spin will dramatically change the nature of the ground state of a few-electron system. We find that the interaction causes drastic changes in the nature of the ground state as the flux varies and that the absence of the exchange interaction for electrons in opposite valleys means that the singlet-triplet degeneracy is not lifted for some states. The extra crossings in the spectrum which are generated by the interaction manifest themselves as steps appearing in the persistent current (the fractional AB effect) and results in intricate structures in the absorption spectrum. These effects are all experimentally measurable. Details of the periods of the oscillations of the persistent current depend on the width of the ring and hence the interplay between kinetic and Coulomb energies.

We use the valley symmetric form of the graphene Hamiltonian¹⁴

$$\mathcal{H} = \tau_0 \otimes \mathcal{H}_0 + \tau_z \otimes \sigma_z V(r), \quad (1)$$

where $V(r)$ is a mass term which describes the confinement of the electron, $\mathcal{H}_0 = v_F(\vec{p} \cdot \vec{\sigma})$ is the bulk graphene Hamiltonian, $\sigma_{x,y,z,0}$ and $\tau_{x,y,z,0}$ are Pauli matrices in the sublattice and valley spaces, respectively, $\vec{p} = -i\hbar\vec{\nabla} + e\vec{A}$, and v_F is the Fermi velocity. The vector potential is taken as $\vec{A} = (\Phi/2\pi r)\vec{e}_\varphi$, where Φ is the total magnetic flux threading the ring. The index N stands for the pair of quantum numbers $[m, \tau]$, where m is the orbital angular momentum and $\tau = +1(-1)$ in the K (K') valley. The single-electron wave function $\psi_N(\rho)$ for a ring of width W and radius R [see Fig.

2(c)] written in terms of the dimensionless radial coordinate $\rho=r/W$ is

$$\psi_N(\rho) = e^{i(m-(1/2))\varphi} b_N \begin{bmatrix} f_N(|\varepsilon_N|\rho) \\ i \operatorname{sgn}(\varepsilon_N) e^{i\varphi} g_N(|\varepsilon_N|\rho) \end{bmatrix}, \quad (2)$$

where

$$f_N = \alpha_N H_{\bar{m}-(1/2)}^{(1)}(|\varepsilon_N|\rho) + H_{\bar{m}-(1/2)}^{(2)}(|\varepsilon_N|\rho),$$

$$g_N = \alpha_N H_{\bar{m}+(1/2)}^{(1)}(|\varepsilon_N|\rho) + H_{\bar{m}+(1/2)}^{(2)}(|\varepsilon_N|\rho),$$

$$\alpha_N = - \frac{H_{\bar{m}-(1/2)}^{(2)}(|\varepsilon_N|\rho_-) + \tau \operatorname{sgn}(\varepsilon_N) H_{\bar{m}+(1/2)}^{(2)}(|\varepsilon_N|\rho_-)}{H_{\bar{m}-(1/2)}^{(1)}(|\varepsilon_N|\rho_-) + \tau \operatorname{sgn}(\varepsilon_N) H_{\bar{m}+(1/2)}^{(1)}(|\varepsilon_N|\rho_-)}$$

with $\rho_{\pm} = \frac{R}{W} \pm \frac{1}{2}$, $\bar{m} = m + \frac{\Phi}{\Phi_0}$, b_N is the normalization factor, and $\operatorname{sgn}(x) = 1$ for $x \geq 0$ and $\operatorname{sgn}(x) = -1$ for $x < 0$. The functions $H_{\nu}^{(1)}(x)$ and $H_{\nu}^{(2)}(x)$ are, respectively, Hankel functions of the first and second kinds.

The ring confinement used to derive Eq. (2) is defined by the mass term [written as the potential $V(r)$] in the Hamiltonian. We employ infinite mass boundary conditions^{14,16} so that $V(r) \rightarrow \infty$ outside the ring. This yields the boundary condition $\psi(\rho_{\pm}) = \tau(\vec{n} \cdot \vec{\sigma})\psi(\rho_{\pm})$. The coefficient α_N is found by applying this condition at the inside edge, an eigenvalue equation for ε_N is derived by subsequently imposing the boundary condition at the outside edge, and b_N is calculated numerically for each state and value of the flux via the normalization condition for the wave function.

The interacting few-electron system is studied by adding the term

$$C = \frac{1}{2} \sum_{i \neq j} \frac{e^2}{4\pi\epsilon_g} \frac{1}{|\vec{r}_i - \vec{r}_j|} \quad (3)$$

to the Hamiltonian where ϵ_g is the dielectric constant of monolayer graphene. This form allows direct interaction between all electrons, but the exchange part is present only between electrons in the same valley and with the same spin as each other. There are no singularities in the matrix elements of this interaction since the band structure of the wave functions introduces a cutoff at small distances, which we take into account only if the corresponding matrix element diverges. The simple matrix structure of this operator is unchanged by the transformation to the valley-symmetric form. We evaluate (numerically) the matrix elements of this operator over the single-particle wave functions in Eq. (2). Using these single-particle matrix elements, we construct the many-body Hamiltonian and carry out an exact diagonalization procedure to determine the energy and eigenstates of the interacting system. The persistent current j is then calculated by taking the derivative of the ground-state energy E_0 of the few-electron system with respect to the flux as $j(\Phi) = \frac{\partial}{\partial \Phi} E_0$.

To describe the absorption of incident light by the graphene ring we add a term to the Hamiltonian which describes the coupling of electrons to the field via the vector potential $\vec{A}_{EM} = 2A_0 \vec{\alpha} \cos(\vec{k} \cdot \vec{r} - \omega t)$. We assume that the radiation propagates as a plane wave with wave vector \vec{k} , frequency ω , and polarization described by the unit vector $\vec{\alpha}$. Then, the Hamiltonian can be written as

$$\mathcal{H} = v_F \vec{\sigma} \cdot (\vec{p} + e\vec{A}_B + e\vec{A}_{EM}) + \tau V(r) \sigma_z + C \quad (4)$$

in the valley-symmetric representation. The transition rate from state N to state N' is calculated from

$$w_{N'N} \propto |\langle N' | \sigma_x \alpha_x + \sigma_y \alpha_y | N \rangle|^2 = 4\pi^2 |I_{N'N}|^2, \quad (5)$$

with

$$I_{N'N} = \int_{\rho_-}^{\rho_+} \rho d\rho b_N^* b_N (\delta_{\tau',K} \delta_{\tau,K} + \delta_{\tau',K'} \delta_{\tau,K'}) [\delta_{m',m+1}(\alpha_x - i\alpha_y) f_{N'}^* g_N - \delta_{m',m-1}(\alpha_x + i\alpha_y) g_{N'}^* f_N] \quad (6)$$

in the dipole approximation. The integral (where we drop the coordinate dependence of the spatial functions for brevity) must be evaluated numerically. The intensity of the absorption is proportional to this transition rate, and the area of the dots in the lowest panels of Figs. 1(a)–1(c) scales with this quantity. In all figures we show the absorption of unpolarized light [i.e., $\vec{\alpha} = (\vec{e}_x + \vec{e}_y)/\sqrt{2}$]. Equation (6) shows that transitions which change the angular-momentum quantum number by ± 1 are permitted so long as the valley index remains unchanged. Where the initial state of a transition is degenerate, we take the average of the intensity of all possible pairs of initial and final states.

In Fig. 1(a) we show the energy spectrum, persistent current, and optical absorption for a single electron in the graphene ring with $R/W = 10$. The lifting of the valley degeneracy previously described causes the step in the persistent current at $\phi = \Phi/\Phi_0 = 0.5$. For $0 < \phi < 0.5$ the ground state consists of one electron in the $m = -\frac{1}{2}$, $\tau = -1$ state whereas for $0.5 < \phi < 1$ the valley index is $\tau = +1$. For $\phi \geq 0$, transitions to the lowest-lying states $m = +\frac{1}{2}$, $\tau = +1$ and $m = -\frac{1}{2}$, $\tau = -1$ are not allowed since the optical absorption cannot mix valleys.

For two noninteracting electrons, the ground state consists of a pair of electrons with antiparallel spins occupying the same single-particle states as in the single-electron system [Fig. 1(b)]. The persistent current reflects the similarity between the ground states of the single particle and $N=2$ noninteracting system, and since there are now two electrons, the persistent current is doubled. The excited states can have varying degrees of degeneracy. If the quantum number pairs $P = [m_P, \tau_P]$ and $Q = [m_Q, \tau_Q]$ of the two electrons are identical then there is only one permitted configuration of the electron spins: the singlet state. However, if $P \neq Q$ then there are four degenerate possibilities: the singlet and three triplet states.

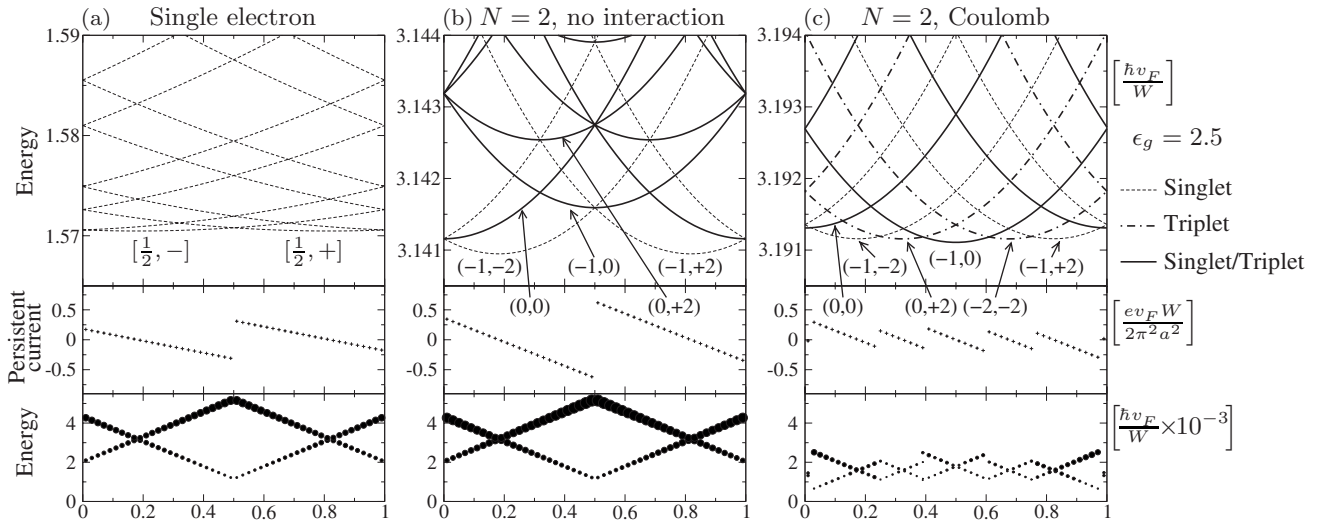


FIG. 1. Energy spectrum (top pane), persistent current (middle pane), and optical absorption of unpolarized light (lower pane) by (a) a single electron, (b) two noninteracting electrons, and (c) two electrons with the Coulomb interaction included. States in the two-electron plots are labeled by the pair of quantum numbers (M, T) where M is the total angular momentum and T is the total valley index. The area of the points in the absorption plots represents the intensity of the peak in arbitrary units. In all three plots, $W=10$ nm and $\frac{R}{W}=10$, and $\epsilon_g=2.5$ (Ref. 17).

When the Coulomb interaction is included [Fig. 1(c)], the picture changes drastically. To describe the two-particle states, we introduce the notation $M=m_1+m_2$ for the total angular momentum and $T=\tau_1+\tau_2$ for the total valley quantum number. The exchange interaction will split the degenerate singlet-triplet states when both of the electrons are in the same valley, i.e., for $T=\pm 2$. In this case, the energy of the singlet does not contain any contribution from exchange and consequently has a rather higher energy than the corresponding triplet. This is exemplified by the $(M=0, T=2)$ state. The triplet part experiences exchange, and this reduces its energy sufficiently for it to form the ground state for $\phi \approx 0.3$ with $\epsilon \approx 3.191$. At the same flux the singlet state has $\epsilon \approx 3.205$ and therefore has energy too high to be shown in Fig. 1(c). On the other hand, the singlet and triplet parts of the $(-1, 0)$ degenerate state are not split by the exchange interaction.

Because the Coulomb matrix elements depend on the angular momenta of the single-electron states involved, the size of the energy change will vary between different few-electron states. This is shown in the vicinity of the crossing of the lowest three states for $\phi=0$. The $M=\pm 1$ states each contain two electrons in the same angular-momentum state ($m=\pm \frac{1}{2}$), so their interaction is stronger than the electrons in the $M=0$ state which has electrons in different angular-momentum states. This causes the ground state to become a degenerate singlet-triplet combination for a small range of flux.

This intricate interplay of different-sized contributions from the Coulomb interaction adds significant complexity to the ground state of the interacting system. In the noninteracting case the ground state is always comprised of a singlet, but the interaction introduces several additional level crossings which give rise to ranges of flux where the ground state becomes a triplet or degenerate singlet-triplet state. More-

over, since the energy due to the Coulomb interaction depends on the angular momentum of the state, the size of the ring will also be an important factor. In Fig. 2(a) we plot the ground-state energy for $\frac{R}{W}=3$ (a wide ring) and 25 (a narrow ring) to illustrate this dependence. The relative depths of the local minima of the ground-state energy are not alike, and the nature of the ground state at zero field changes from the $(-1, -2)$ singlet in a wide ring to the $(0, 0)$ singlet-triplet in a narrow ring. This transition is revealed by the absorption spectrum, since the crossover to the degenerate ground state changes the spectrum to two closely spaced low intensity peaks. In Fig. 2(b), the difference in energy between $(0, 0)$ and $(-1, -2)$ is plotted as a function of $\frac{R}{W}$ for a ring with $R=100$ nm. The crossover for the ground state occurs at approximately $\frac{R}{W}=7$, which is independent of the value of R .

For three noninteracting electrons in the ring, the ground state is composed of spin and valley states with minimal

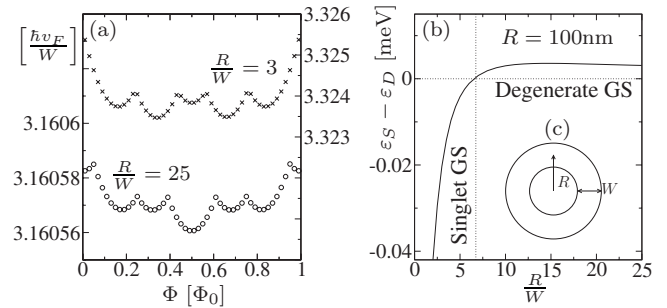


FIG. 2. The effect of the ring width on the ground-state energy. (a) The $\frac{R}{W}=3$ curve (crosses) is plotted relative to the right-hand axis, and the $\frac{R}{W}=25$ curve (circles) is plotted relative to the left-hand axis. (b) The energy difference between lowest singlet (ϵ_S) and degenerate singlet-triplet (ϵ_D) states at $\Phi/\Phi_0=0$. (c) The geometry of the ring.

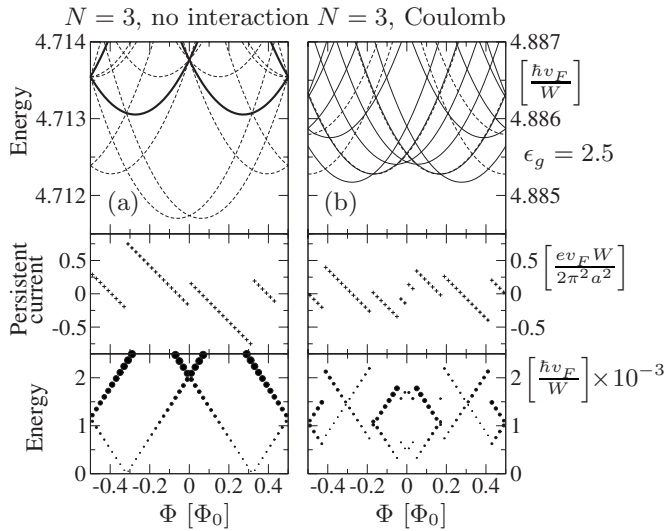


FIG. 3. (a) Noninteracting and (b) interacting three-electron energy spectra, persistent current, and optical absorption for $\frac{\hbar v_F}{W} = 10$. Dashed lines denote twofold degeneracy, solid lines denote fourfold degeneracy, and thick solid line denotes eightfold degeneracy of the state.

polarization (i.e., $T = \pm 1$) (Fig. 3). When the interaction is added, the contribution from exchange is largest for $T = \pm 3$ states so the low-energy spectrum becomes much more compact, just as in the $N=2$ case. Qualitatively, the effect of the

interaction is the same as previously, so the changing nature of the ground state again demonstrates the complexity due to the absence of the valley degeneracy. However, because there are more possible combinations of states, the persistent current and absorption spectrum are correspondingly more complex in their structure. In particular it is not possible to have $T=0$ so the exchange energy is always finite. However, its contribution is larger for $T = \pm 3$ states than for $T = \pm 1$ states. It is also the case that the width of the ring (and hence the relative strength of the interaction) will affect the detail of the ground state.

To summarize, we have studied the effect of the electron-electron interaction on measurable quantities in a graphene quantum ring. We find that the interplay of the interaction and the total valley quantum number allow for an intricate manifestation of the breaking of valley degeneracy in this geometry. The change of the interacting ground state between singlet, triplet, and degenerate singlet-triplet natures reveals the sensitivity of the exchange contribution to the total valley index. These changes in the ground state are manifested in the fractional nature of the AB oscillations in the persistent current, and in the steps and intensity changes in the absorption spectrum as the flux is varied.

This work has been supported by the Canada Research Chairs Program and the NSERC Discovery Grant, and we would like to thank P. Pietiläinen for helpful discussions.

*abergel@cc.umanitoba.ca

†chakrabort@cc.umanitoba.ca

¹K. S. Novoselov, A. K. Geim, S. V. Morozov, D. Jiang, Y. Zhang, S. V. Dubonos, I. V. Grigorieva, and A. A. Firsov, *Science* **306**, 666 (2004); For recent works, see V. I. Fal'ko, B. Altschuler, and I. Aleiner, *Eur. Phys. J. Spec. Top.* **148**, 1 (2007); S. Das Sarma, P. Kim, A. K. Geim, and A. H. MacDonald, *Solid State Commun.* **143**, 1 (2007).

²P. R. Wallace, *Phys. Rev.* **71**, 622 (1947).

³A. K. Geim and K. S. Novoselov, *Nature Mater.* **6**, 183 (2007).

⁴Y. Zhang, Z. Jiang, J. P. Small, M. S. Purewal, Y. W. Tan, M. Fazlollahi, J. D. Chudow, J. A. Jaszczak, H. L. Stormer, and P. Kim, *Phys. Rev. Lett.* **96**, 136806 (2006).

⁵T. Chakraborty and P. Pietiläinen, *Europhys. Lett.* **80**, 37007 (2007); J. Alicea and M. P. A. Fisher, *Phys. Rev. B* **74**, 075422 (2006); K. Nomura and A. H. MacDonald, *Phys. Rev. Lett.* **96**, 256602 (2006); J. N. Fuchs and P. Lederer, *ibid.* **98**, 016803 (2007).

⁶M. Büttiker, Y. Imry, and R. Landauer, *Phys. Lett.* **96**, 365 (1983); F. von Oppen and E. K. Riedel, *Phys. Rev. Lett.* **66**, 84 (1991).

⁷Y. Aharonov and D. Bohm, *Phys. Rev.* **115**, 485 (1959).

⁸T. Chakraborty and P. Pietiläinen, *Phys. Rev. B* **50**, 8460 (1994); V. Halonen, P. Pietiläinen, and T. Chakraborty, *Europhys. Lett.* **33**, 377 (1996).

⁹A. Lorke, R. J. Luyken, A. O. Govorov, J. P. Kotthaus, J. M. Garcia, and P. M. Petroff, *Phys. Rev. Lett.* **84**, 2223 (2000).

¹⁰A. Fuhrer, S. Lüscher, T. Ihn, T. Heinzel, K. Ensslin, W. Wegscheider, and M. Bicher, *Nature (London)* **413**, 822 (2001).

¹¹K. Niemelä, P. Pietiläinen, P. Hyvönön, and T. Chakraborty, *Europhys. Lett.* **36**, 533 (1996).

¹²U. F. Keyser, C. Fuhner, S. Borck, R. J. Haug, M. Bichler, G. Abstreiter, and W. Wegscheider, *Phys. Rev. Lett.* **90**, 196601 (2003).

¹³S. Russo, J. B. Oostinga, D. Wehenkel, H. B. Heersche, S. S. Sobhani, L. M. K. Vandersypen, and A. F. Morpurgo, *Phys. Rev. B* **77**, 085413 (2008); K. Ensslin (private communication).

¹⁴P. Recher, B. Trauzettel, A. Rycerz, Y. M. Blanter, C. W. J. Beenakker, and A. F. Morpurgo, *Phys. Rev. B* **76**, 235404 (2007).

¹⁵A. Rycerz and C. W. J. Beenakker, arXiv:0709.3397 (unpublished).

¹⁶M. V. Berry and R. J. Mondragon, *Proc. R. Soc. London, Ser. A* **412**, 53 (1987); E. McCann and V. I. Fal'ko, *J. Phys.: Condens. Matter* **16**, 2371 (2004); J. Tworzydło, B. Trauzettel, M. Titov, A. Rycerz, and C. W. J. Beenakker, *Phys. Rev. Lett.* **96**, 246802 (2006); P. G. Silvestrov and K. B. Efetov, *ibid.* **98**, 016802 (2007).

¹⁷T. Ando, *J. Phys. Soc. Jpn.* **75**, 074716 (2006).